IEEE Access
Multidisciplinary ⋮ Rapid Review ⋮ Open Access Journal

Received 9 August 2023, accepted 3 September 2023, date of publication 14 September 2023,
date of current version 22 September 2023.

Digital Object Identifier 10.1109/ACCESS.2023.3315318

RESEARCH ARTICLE

Shape Memory Alloy-Based Fluidically Reconfigurable Metasurfaced Beam Steering Antenna

SYED IMRAN HUSSAIN SHAH[1], SAYED SABIR SHAH[2], EIRÍKUR BERNHARÐSSON[3], AND SLAWOMIR KOZIEL[1,3], (Fellow, IEEE)

[1]Faculty of Electronics, Telecommunication and Informatics, Gdańsk University of Technology, 80-233 Gdansk, Poland
[2]Department of Electrical Engineering, University of Engineering and Technology Peshawar, Peshawar 25000, Pakistan
[3]Department of Engineering, Reykjavik University, 102 Reykjavik, Iceland

Corresponding author: Syed Imran Hussain Shah (engr.shahsyedimran@gmail.com)

This work was supported in part by the National Science Centre of Poland under Grant 2020/37/B/ST7/01448, and in part by the Icelandic Centre for Research (RANNIS) under Grant 206606.

ABSTRACT A low-cost actuator-based fluidically programmable metasurface (FPMS) antenna is proposed to solve the slow tuning speed problem of the manually fluidic based reconfigurable antennas. The FPMS-based antenna is probe-fed and comprises a 4×4 square ring metasurface as a superstrate. Moreover, two shape memory alloy (SMA)-based electrically-controlled actuators are employed in the design for controlling the position of the 3D-printed fluidic channels beneath the metasurface along the axes of the radiating slots of the patch antenna. This results in beam-steering of over $\pm 20°$ in the elevation plane, with a peak gain of 9.1 dBi. It is worth mentioning that compared to conventional electronic tuning technologies where the switches are employed on the top of the radiating aperture of the antenna, which usually deteriorate the antenna performance, the SMA spring actuators do not deteriorate the performance as these are not interacting with the radiating aperture. The proposed antenna was designed and simulated using CST MWS, and the prototype was fabricated and measured. The simulated and measured results are in good agreement, which corroborates the adequacy of the proposed concept. By incorporating the SMA-based fluidic actuators, the proposed antenna is simple and highly efficient as compared to metasurface-based beam-steering antennas reported in the literature thus far.

INDEX TERMS Shape memory spring actuators, metasurface, fluidic antennas, beam-steering antenna, fluidically programmable metasurface (FPMS).

I. INTRODUCTION

Reconfigurable antennas are in the limelight due to their multiple functionalities obtained from a single structure. These antennas have the ability to switch either their frequency, pattern, polarization or any combination of these, called compound/hybrid reconfiguration. In particular, pattern reconfigurable antennas can be designed by various techniques. Among these, metasurfaces, which are planar two-dimensional counterparts of metamaterials, are getting considerable attention due to their electromagnetic wave focusing capability as well as being planar and exhibiting a compact structure [1]. Different kinds of beam switching techniques such as electronic tuning using PIN diode [2], [3], [4], [5], [6] varactor-diode [7], [8] barium strontium titanate (BST), and micro-electro-mechanical system (MEMS) switching have been employed in metasurfaces [3], [8], [9], [10], [11], [12], [13].

In the existing literature, numerous metasurface-based high-gain antennas with beam steering capabilities have been reported [14], [15], [16], [17], [18]. However, these designs exhibit certain limitations such as low power handling capacity, low system efficiency, inadequate switch isolation, complex biasing networks, unfavorable noise behavior,

The associate editor coordinating the review of this manuscript and approving it for publication was Pavlos I. Lazaridis.

which need to be addressed from the point of view of practical applications. For instance, the antenna reported in [14] comprises three stacked substrates with air gaps between the top two layers. Metasurfaces on the upper and the lower layers are connected through vias, exhibiting good performance, despite a complex design due to its multilayer configuration. A low-cost 3D-printed metasurface antenna with beam steering capability has been reported in [15]; however, efficiency of the antenna is only 21%. Similarly, in [16] a multilayer beam steering metasurface antenna has been reported, however, design of the antenna is somehow complicated. Additionally, the use of a large number of PIN diodes in certain designs introduces insertion losses and non-linearities [17], whereas certain structures require complex biasing techniques [18]. Even when a metasurface with a combination of active and passive metaatoms is employed to reduce the number of PIN diodes, the required quantity remains considerable, such as 24, and the beam steering capability is limited to only 10° [18].

In pursuit of overcoming the limitations of active metasurface antennas, alternative approaches have been explored, such as utilizing gallium liquid metal alloy, and dielectric fluids [19], [20], [21], [22], [23]. These fluid-based metasurface antennas exhibit advantages, yet they also face challenges. For instance, manual control of fluidic channels can result in slower tuning speeds of the antenna [24]. While some studies have used micropumps to improve the tuning speed, this solution requires multiple high cost micropumps, which can be detrimental to the benefits of this tuning technique [24], [25]. Furthermore, the antenna cannot be remotely tuned [22]. In addition, a micropump requires additional effort and costly control units, which makes the overall system expensive and complex.

To overcome the aforementioned limitations, a simplified, shape-memory-actuator-based fluidically programmable metasurface (FPMS) antenna is presented in this work. Instead of manual filling and evacuating the fluidic channels, we employed two shape memory alloy (SMA) spring actuators for programming the position of the 3D-printed fluidic channels beneath the metasurface, as illustrated in Fig. 1. Adjusting the fluidic channels position along the radiating slots of the patch contributes to a near-field phase transformation due to high permittivity of water, thereby enabling continuous beam steering within a range of more than ±20° in the azimuth plane. This allows us to overcome the issue of slow tuning speed pertinent to manually reconfigurable antennas. The proposed actuators possess moderate tuning speed and are slower than other tunable and switchable microwave devices. However, this actuation-based switching technique is useful for applications where periodic structures are utilized, and large number of diodes are required with complicated biasing circuits, such as tunable or reconfigurable metasurfaces [2], [3], [8], [26], [27], [28], [29]. For instance, in [30], 144 pin diodes are employed to design a partial reflective surface (PRS)-based reconfigurable antenna, which makes the structure lossy and complex. Since the SMA actuators are situated underneath the metasurface, they do not interact with the metasurface, which eliminates insertion losses present in conventional microwave switches. To the best of authors' knowledge, no similar technique for beam steering has been previously published in the literature.

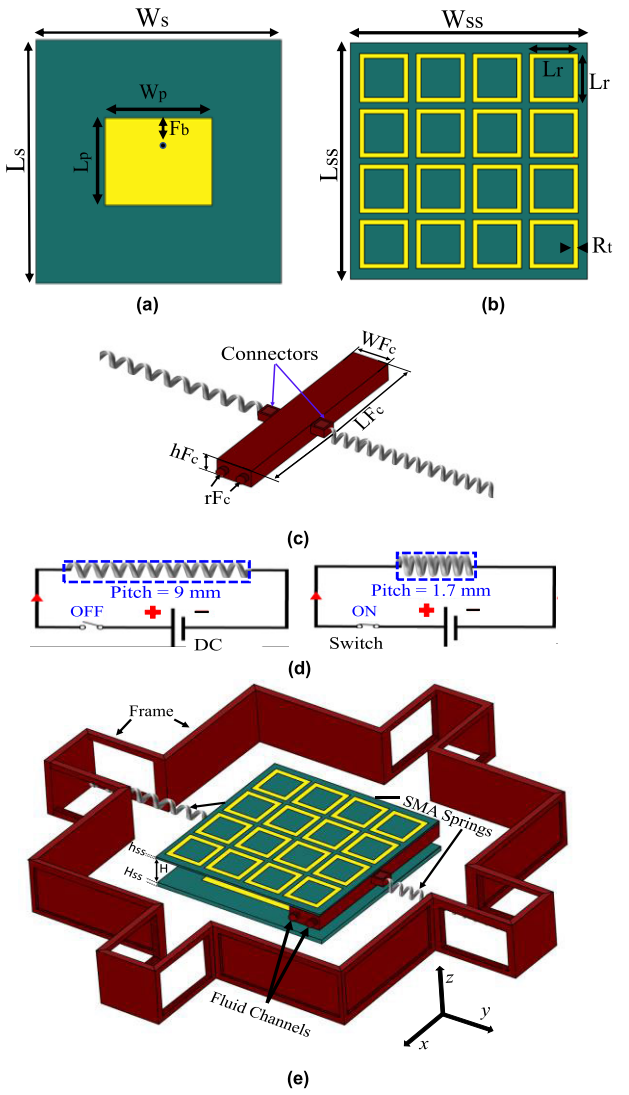

FIGURE 1. Structure of the Proposed design (a) probe fed patch antenna, (b) metasurface design, (c) water filled fluidic channels, (d) SMA actuators pitch variation (e) final antenna design.

II. ANTENNA DESIGN

A. PROPOSED CONCEPT

The proposed antenna consists of a rectangular patch fed by a coaxial probe located at a distance F_b from the patch side. The patch dimensions are $L_p \times W_p$. The antenna is designed on Arlon AD250 substrate ($\varepsilon_r = 2.5$, loss tangent 0.0018) with dimensions of $L_s \times W_s \times h_s$, as shown in Fig. 1(a). The Antenna consists of a superstrate with the size $L_{ss} \times W_{ss} \times h_{ss}$ which is at a distance H from the patch center and includes 4×4 square ring unit cells also designed on Arlon AD250

substrate of thickness h_{ss} as shown in Fig. 1(b). The proposed design also consists of the two SMA springs, which are attached to the water-filled fluidic channels (FCs) as shown in Fig. 1(c). The SMA springs can be elongated by use of an external force while they can be recompressed by applying a certain voltage as shown in Fig. 1(d.). Moreover, the FCs are designed using polylactic acid (PLA) material ($\varepsilon_r = 2.5$, loss tangent 0.002). The dimensions of the proposed design are summarized in Table 1. Furthermore, the antenna consists of 3D printed holder to connect antenna, fluidic channels, metasurface and SMA actuators as shown in Fig. 1(e).

TABLE 1. Dimensions of the proposed antenna.

L_s	W_s	L_{ss}	W_{ss}	L_p	W_p
85	85	85	85	47.24	38.89
H	H_{ss}	h_{ss}	F_b	L_r	R_t
14.03	1.52	0.76	7.44	18	1
LF_c	WF_c	hF_c	rF_c		
80	20	10	2		

All values are in mm

B. FLUIDIC CHANNELS PROGRAMMING MECHANISM

The switchable phase of the metasurface was obtained by controlling the position of the 3D-printed fluidic channels beneath the metasurface, which contributes to the phase change and directing the beam to a particular direction as shown in Fig. 2(a). The FCs are filled with tap water ($\varepsilon_r = 80$, $\tan\delta = 0.04$). To program the FCs position along the radiating slots of the patch antenna, two SMA actuators are attached. As the SMA springs possess one-way memory, to enable bidirectional movement, two springs are attached back-to-back. As an example, with a pair of springs, the compression of SMA spring actuator #1 by a bias voltage along the $+y$ or $-y$ directions will lead to automatic expansion of SMA spring actuator #2 along that direction, whereas the fluidic channels will be relocated in the y-direction. Thus, the y-direction spring pair exhibits forward and reverse movements simultaneously. When FCs are at the center, represented by P0, the antenna radiates in the broadside direction. As we program the position of the FCs across the patch for values such as P1, P2, P3, P4, the beam tilting increases gradually by 2°, 6°, 14°, 21° and 24°, symmetrically for both left side (LS) and right side (RS) directions, which is illustrated in Fig. 2(b).

C. SMA ACTUATOR CHARACTERIZATION

In the proposed design, the position of the fluidic channels was programmed by DC excitation of the SMA electromechanical spring actuators to achieve beam steering capability. SMA actuators are thin contraction-type helical structures, which can be deformed and elongated at the room temperature by applying the external force, whereas it can be restored and recompressed to its original shape by passing direct current through it. For instance, in the employed SMA model, the length can be varied by 78% and it can be stretched to

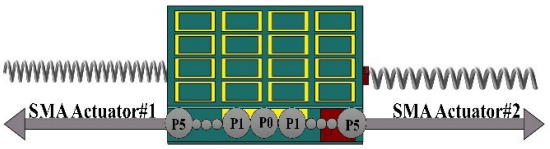

Position	P0	P1	P2	P3	P4	P5
Distance from Center of Patch (mm)	0	6	12	18	24	30
SMA Spring Actuator#1 Pitch (mm)	6.9	6.9	8.2	8.2	9.5	9.5
SMA Spring Actuator#2 Pitch (mm)	5.2	5.2	3.9	3.9	2.6	2.6
Beam steering (Degrees)	2°	6°	14°	21°	24°	20°

(a)

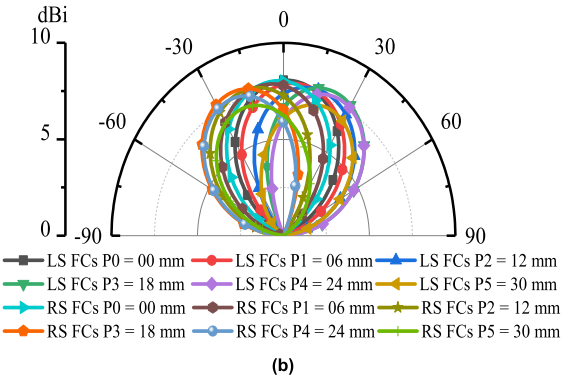

(b)

FIGURE 2. (a) Programming position of water filled fluidic channels, (b) beam steering of the antenna.

150 mm (which is about 30 mm in the compressed state), and it exerts a force of 10 Newton during contraction. This pulling force is used for the movement/programming of the fluidic channels beneath the metasurface.

In the present study, an SMA spring with a pitch (distance between two successive turns) of 9 mm having total length of 150 mm was chosen, and an external DC excitation voltage in the range of 0.7–2 V with 3 A current was applied to the two open ends of the spring. Detailed characterization process of the SMA actuator can be found in [31] and [32], where it is demonstrated that SMA actuators show stable performance after repeated usage.

The effects of the additional associated elements of the proposed design, such as the 3D frame, empty and water filled fluidic channels, and SMA springs, on the reflection coefficients and radiation patterns were studied thoroughly. Initially, the reflection coefficients of the source antenna with and without the metasurface were studied, as presented in Fig. 3(a). The resonant frequency of the source antenna without and with the metasurface is 2.33 and 2.42 GHz, respectively. Further, the effects of 3D-printed empty and water filled fluidic channels, the 3D-printed holder frame and SMA are analysed and included in Fig. 3(a). These additional components have a slight effect on the resonant frequency and the impedance bandwidth. However, it is noteworthy, that the SMA actuators do not have a significant effect on

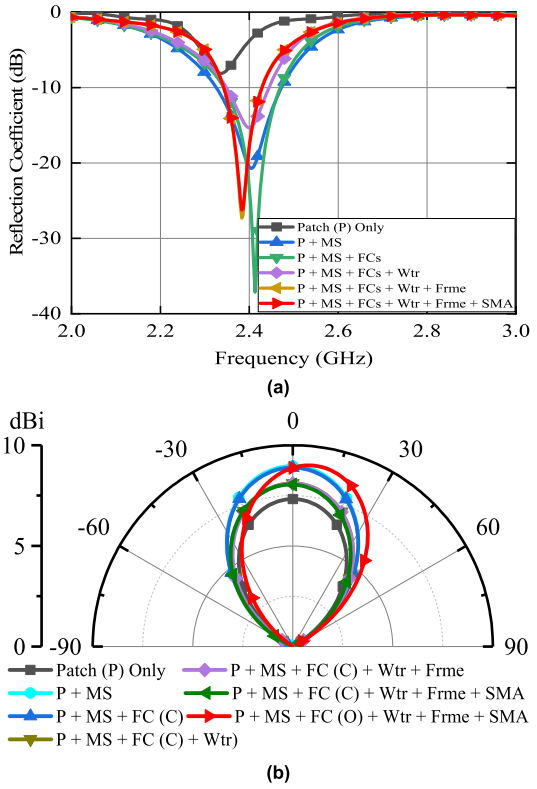

FIGURE 3. Effect of additional associated elements of the proposed design (a) on reflection coefficient, (b) on radiation performance.

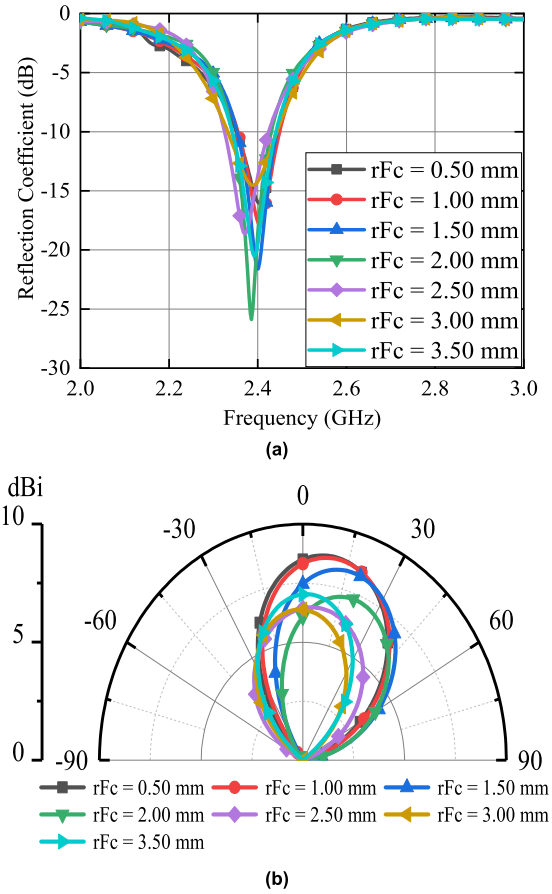

FIGURE 4. Effect of radius of water filled fluidic channels on (a) reflection coefficient and (b) beam steering capability of the proposed design.

antenna performance in terms of the impedance matching and resonant frequency.

The effect of the abovementioned additional associated elements are also analysed in terms of the antenna radiation patterns and demonstrated in Fig. 3(b). It can be seen that the metasurface increased the gain of simple patch antenna by 2 dB. However, water-filled fluidic channels decreased the antenna gain by 1.63 dB owing to the lossy nature of the water. In addition, it is worth to mention that empty fluidic channels, frame and SMA does not have any impact on antenna performance. Similarly, the water-filled channels, when they are outside the cavity/vicinity of metasurface, do not degrade antenna performance either.

D. DESIGN EVOLUTION

As discussed, the effect of various components on S-parameters and radiation pattern can be observed in Fig. 3(a) and Fig. 3(b) respectively. It can be seen that the proposed design evolved through a number of iterations/steps during simulations. First, a rectangular patch is designed with the required dimensions. Subsequently, a 4 × 4-unit cell metasurface is integrated at an optimum distance H from the patch surface to enhance the gain of the antenna by approximately 2 dB. Then, a 3D-printed PLA substrate having FCs for constraining liquid is integrated to observe the response. In the next stage, the FCs are filled with tap water to observe the response whilst two SMA spring attached to the periphery of the FCs and frame to relocate the channels across the patch. Similarly, the effects of the fluidic channel radius on antenna responses are analyzed in terms of matching and corresponding beam tilting. Fig. 4(a) indicates that proposed value of water channel radius (rFc) of 2 mm ensures the best possible matching. At the same time, Fig. 4(b) demonstrates that rFc = 2 mm results in a maximum beam tilt and an optimal gain. There is a tradeoff between gain and beam tilting as shown by Fig. 4. At rFc = 1.5mm the gain value is 8.26 dBi while beam tilt is 17°. For rFc = 2 mm the beam tilt is 21° and gain is 7.26 dBi. So, keeping in view the desired performance, we choose an optimal value of rFc which is most suitable to our requirements.

III. RESULTS AND DISCUSSION

The proposed design has been fabricated and experimentally validated, cf. Fig. 5 and Fig. 6 respectively. The patch antenna and metasurface are fabricated on Arlon AD250 substrate, both having similar dimensions of 85 mm × 85 mm × 1.524 mm as depicted in Figs. 5(a) and 5(b) respectively. The FCs contain tap water as dielectric material with relative permittivity of $\varepsilon_r = 80$ and $\tan\delta = 0.04$. The FCs and the PLA frame are fabricated using an SLA 3D printing technique, which are shown in Fig. 5(c) and 5(d) respectively.

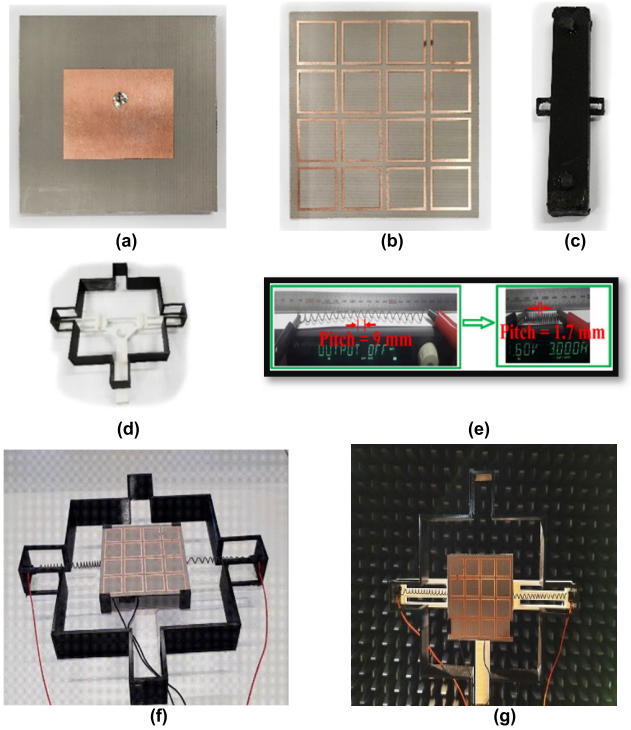

FIGURE 5. Fabricated prototype of the proposed antenna and antenna elements (a) patch antenna, (b) metasurface, (c) fluidic channels, (d) PLA frame with holder (to attach the structure to the measurement tower within the anechoic chamber, (e) SMA actuator DC biasing [31], (f) complete setup with actuators, (g) antenna in the anechoic chamber.

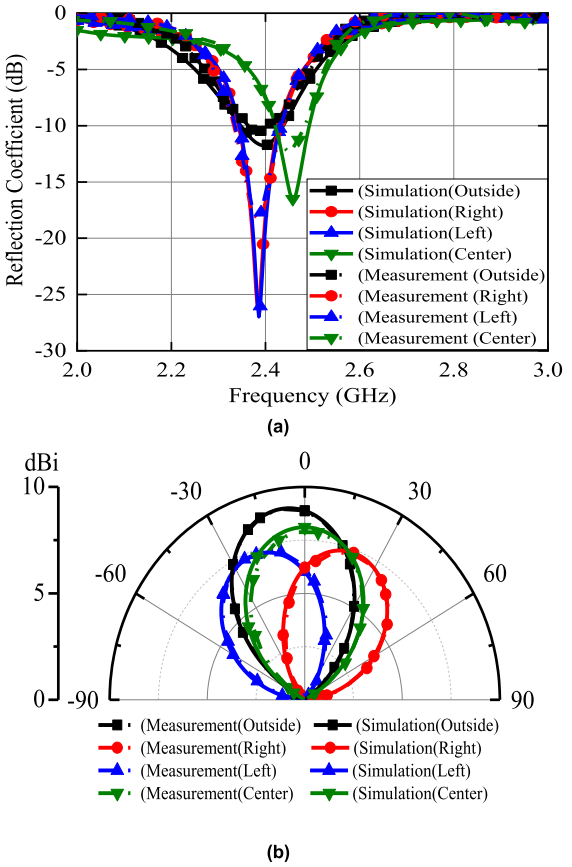

FIGURE 6. Comparison of simulated and measured results for different positions of fluidic channels in terms of (a) reflection coefficients, (b) radiation patterns.

This results in prints that are smooth and impermeable as compared to the frequently used FDM printings. The SMA actuator is expanded and contracted by the application of small DC voltage which can be observed in Fig. 5(e). In the prototype, one end of the SMA spring is attached to FCs, whereas the other is attached to the PLA frame as depicted in Figs. 5(f) and 5(g) respectively. In order to control the position of the FCs, a DC voltage in the range of 0.7 V to 2 V is applied to compress the spring from one side. A relatively large size of the antenna system is due to the employment of the larger size SMA actuators available at [33], which are low cost and readily available, and therefore employed to demonstrate the proof of concept of the proposed antenna. Nevertheless, several types of SMA springs with compact sizes are reported for various applications [34], [35], [36]. Their employment will be one of the objectives of the future work aiming at size reduction of the presented antenna system.

Figures 6(a) and 6(b) show a comparison between the simulated and measured antenna characteristics, specifically, S-parameters and radiation patterns, respectively. In both graphs, the solid lines represent the simulated results, whereas the dash-dot lines represent the measured results. It could be observed that the simulated and measured results are in remarkably good agreement, with both graphs closely overlapping. The simulated and measured reflection coefficients corresponding to different positions of the fluidic channels (FCs) are shown in Fig. 6(a) which shows close resemblance. The plots indicate that for FCs outside the metasurface, the resonant frequency changes due to high dielectric constant of water. On the other hand, there is a slight increase in resonant frequency when the fluidic channels are at center of the patch. The simulated and measured gain are in a good agreement as illustrated in Fig. 6(b). It can also be observed that a maximum realized gain of 9.1 dBi is obtained when the FCs are outside the metasurface while a maximum achieved gain is 8 dBi for center case. The beam steering behavior, here demonstrated for four scenarios (FC on the left, right, outside, and in the center), can be observed in Fig. 6(b) as well. The maximum simulated beam tilt of 24°, and it is obtained for the fluidic channels at position P4 (cf. Fig. 2).

The gain of the proposed antenna has been shown in Fig. 7(a). The simulated and measurement results are in good agreement at the target operating frequency of 2.4 GHz. A slight discrepancy between the simulated and measured results can be observed at higher frequencies, possibly associated with the lossy nature of water-filled fluidic channels. In Fig. 7(b), the radiation efficiency is plotted to see the effect of different associated elements of the proposed design, where the FCs (Inside) implies the location of fluidic

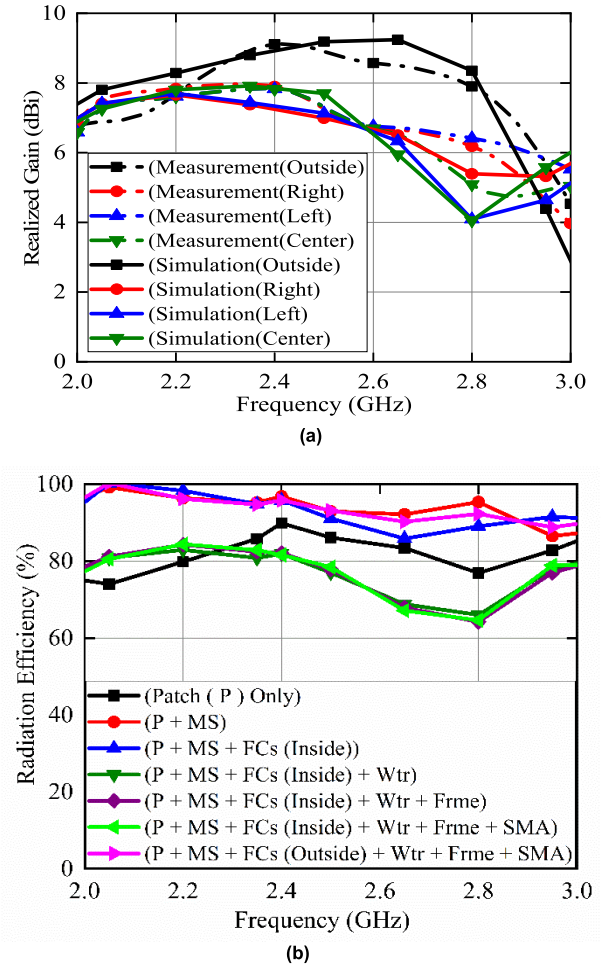

FIGURE 7. Effect of various associated antenna elements on (a) antenna gain (b) radiation efficiency of the proposed design.

channels at left, right and center of cavity of patch and MS while FCs (Outside) implies to the location outside the cavity of patch and MS. It can be observed that efficiency is at its peak when water (Wtr) is not present in FCs and when the FCs is positioned outside the metasurface (MS). However, with the addition of water in the FCs the efficiency drops from approximately 96% to 82%, which is due to the very high dielectric constant of the water. In addition, the effect of other elements such as PLA substrate frame (Frme) and Ni/Ti alloy SMA spring has been analyzed and depicted in the radiation efficiency graph of Fig. 7(b).

It has been found that the SMA springs along with the associated circuitry have negligible effect on the radiation performance of the antenna compared to reconfigurable antennas employing other methods of reconfigurability [3], [9], [37]. From this study, it can be observed that the efficiency of the proposed design is more than 80% at the desired band of 2.4 GHz at all states.

Tables 2 and 3 compare the proposed antenna with state-of- the-art designs from the literature. From Table 2, it can be seen that our design is superior in terms of efficiency, while

TABLE 2. Comparison of proposed design with state-of-the-art metasurface-based designs.

Ref.	Freq (GHz)	Switching Technique	Scanning	Gain (dBi)	Efficiency (%)	Switching Speed
[4]	5.5	PIN	±15°	12	NA	Fast
[5]	2.4	PIN	±30°	4.9	70	Fast
[6]	5.5	PIN	±36	NA	NA	Fast
[10]	5.5	manually	±32°	7.2	85	Low
[20]	7.5	EGaIn	±45°	NA	NA	Low
[22]	2.6	Water	±20°	5.7	55	Low
[41]	2	Varactor	±10°	13	NA	Fast
[42]	5.5	Varactor	±25°	14	<75	Fast
[43]	7.9	Varactor	±7°	NA	NA	Fast
[44]	12	Microfluidics	5°	NA	NA	Low
This work	**2.4**	**SMA**	**±22°**	**9.1**	**82**	**Moderate**

TABLE 3. Comparison of proposed design with state-of-the-art actuator-based designs.

Ref	Tuning Feature	Switching time (sec)	Tuning Speed (mm/s)	Displacement (mm)	Min. Efficiency (%)	Actuator Cost ≅
[38]	Pattern	30	1	30	86	$26.38
[25]	Frequency	20	2.5	50	65	$650
[24]	Frequency	NA	NA	NA	79	NA
[39]	Frequency	12	1.7	NA	53.6	NA
[40]	Frequency	NA	NA	NA	NA	$28.12 to $34.82
This work (Actuator only)	-	16	7.5	150	NA	$7.8
This work (Antenna system)	Pattern	15	4	60	80	$15.6

attaining a maximum gain of 9.1 dBi and beam tilting of 22°. Although, it may be slow in terms of the switching speed as compared to PIN-diode- and varactor-diode-based antennas, the latter require complex biasing circuitry contributing to losses and degradation of the antenna aperture radiation. At the same time, the proposed actuatorbased beam steering technique solve the slow tuning speed issues of manually reconfigurable antennas. Table 3 shows a comparison of the proposed actuator-based reconfigurable antenna with state-of-the-art reconfigurable antennas [24], [25], [38], [39], [40], where the actuators are employed for switching purposes.

The advantages of the proposed actuator include simplicity, robustness and the ease of integration and assembly compared to previous manual fluidically beam steering antenna reported in [22]. In addition, compared to [22], the proposed design is superior in terms of gain and efficiency. It exhibits a continuous beam steering ability. Further, employing SMA springs results in negligible effect on the radiation performance of the antenna. Moreover, the proposed design features

over 80% efficiency at the desired band at all states, and it is cost-efficient as well. The proposed antenna system demonstrates substantial improvements in performance, stability, and handling as compared to [22] and other existing fluidic-based reconfigurable antennas [19], [20], [21], [23], including practical aspects of reconfiguration.

IV. CONCLUSION

In this paper, a shape memory alloy-based fluidically reconfigurable metasurfaced beam steering antenna is presented. Continuous beam switching of more than twenty degrees was achieved by programming the fluidic channels between the patch and metasurface. This technique overcome the slow tunning speed issues of fluidically, manually, as well as other type of actuators based reconfigurable antennas. As the SMA actuators are not in direct contact with the radiating aperture of the antenna, radiation characteristics such as radiation efficiency and gain of the antenna are not degraded. This method allows the antenna to be remotely tuned in contrast to other fluidic based manually reconfigurable antennas. With the ongoing advancements in the materials of SMA actuators, it is expected that the tuning speed will be further increased in the near future. The compact SMA springs are available in [45] and [46], the employment of which requires further research to evaluate their suitability for higher frequency RF applications.

REFERENCES

[1] H. H. Tran, C. D. Bui, N. Nguyen-Trong, and T. K. Nguyen, "A wideband non-uniform metasurface-based circularly polarized reconfigurable antenna," *IEEE Access*, vol. 9, pp. 42325–42332, 2021.

[2] M. Bouslama, M. Traii, T. A. Denidni, and A. Gharsallah, "Beam-switching antenna with a new reconfigurable frequency selective surface," *IEEE Antennas Wireless Propag. Lett.*, vol. 15, pp. 1159–1162, 2016.

[3] D. Rodrigo, B. A. Cetiner, and L. Jofre, "Frequency, radiation pattern and polarization reconfigurable antenna using a parasitic pixel layer," *IEEE Trans. Antennas Propag.*, vol. 62, no. 6, pp. 3422–3427, Jun. 2014.

[4] L.-Y. Ji, Y. J. Guo, P.-Y. Qin, S.-X. Gong, and R. Mittra, "A reconfigurable partially reflective surface (PRS) antenna for beam steering," *IEEE Trans. Antennas Propag.*, vol. 63, no. 6, pp. 2387–2395, Jun. 2015.

[5] M. Li, S.-Q. Xiao, Z. Wang, and B.-Z. Wang, "Compact surface-wave assisted beam-steerable antenna based on HIS," *IEEE Trans. Antennas Propag.*, vol. 62, no. 7, pp. 3511–3519, Jul. 2014.

[6] Y. F. Cao and X. Y. Zhang, "A wideband beam-steerable slot antenna using artificial magnetic conductors with simple structure," *IEEE Trans. Antennas Propag.*, vol. 66, no. 4, pp. 1685–1694, Apr. 2018.

[7] J. Yu, W. Jiang, and S. Gong, "Low-RCS beam-steering antenna based on reconfigurable phase gradient metasurface," *IEEE Antennas Wireless Propag. Lett.*, vol. 18, no. 10, pp. 2016–2020, Oct. 2019.

[8] J. Hu, S. Lin, and F. Dai, "Pattern reconfigurable antenna based on morphing bistable composite laminates," *IEEE Trans. Antennas Propag.*, vol. 65, no. 5, pp. 2196–2207, May 2017.

[9] L. Santamaria, F. Ferrero, R. Staraj, and L. Lizzi, "Electronically pattern reconfigurable antenna for IoT applications," *IEEE Open J. Antennas Propag.*, vol. 2, pp. 546–554, 2021.

[10] H. L. Zhu, S. W. Cheung, and T. I. Yuk, "Mechanically pattern reconfigurable antenna using metasurface," *IET Microw., Antennas Propag.*, vol. 9, no. 12, pp. 1331–1336, Sep. 2015.

[11] Y.-H. Qian and Q.-X. Chu, "A polarization-reconfigurable water-loaded microstrip antenna," *IEEE Antennas Wireless Propag. Lett.*, vol. 16, pp. 2179–2182, 2017.

[12] J. P. Turpin, J. A. Bossard, K. L. Morgan, D. H. Werner, and P. L. Werner, "Reconfigurable and tunable metamaterials: A review of the theory and applications," *Int. J. Antennas Propag.*, vol. 2014, pp. 1–18, 2014.

[13] L. Sumana and S. E. Florence, "Pattern reconfigurable microstrip patch antenna based on shape memory alloys for automobile applications," *J. Electron. Mater.*, vol. 49, no. 11, pp. 6598–6610, Nov. 2020.

[14] J. Luo, L. Li, J. Su, R. Ma, G. Han, and W. Zhang, "Multibeam antenna based on partially reflecting defected metasurface," *IEEE Antennas Wireless Propag. Lett.*, vol. 20, no. 8, pp. 1582–1586, Aug. 2021, doi: 10.1109/LAWP.2021.3091608.

[15] F. Ahmed, T. Hayat, M. U. Afzal, S. Zhang, K. P. Esselle, and W. G. Whittow, "3-D printable synthetic metasurface to realize 2-D beam-steering antenna," *IEEE Open J. Antennas Propag.*, vol. 4, pp. 506–519, 2023, doi: 10.1109/OJAP.2023.3274782.

[16] A. Verma, R. K. Arya, and S. N. Raghava, "Metasurface superstrate beam steering antenna with AMC for 5G/WiMAX/WLAN applications," *Wireless Pers. Commun.*, vol. 128, no. 2, pp. 1153–1170, Jan. 2023, doi: 10.1007/S11277-022-09993-4.

[17] Z. S. Muqdad, M. Alibakhshikenari, T. A. Elwi, Z. A. A. Hassain, B. S. Virdee, R. Sharma, S. Khan, N. T. Tokan, P. Livreri, F. Falcone, and E. Limiti, "Photonic controlled metasurface for intelligent antenna beam steering applications including 6G mobile communication systems," *AEU-Int. J. Electron. Commun.*, vol. 166, Jul. 2023, Art. no. 154652, doi: 10.1016/J.AEUE.2023.154652.

[18] A. H. Naqvi and S. Lim, "Low-profile electronic beam-scanning metasurface antenna for Ka-band applications," *Waves Random Complex Media*, pp. 1–16, Jan. 2023, doi: 10.1080/17455030.2023.2166153.

[19] T. Qian, "Reconfigurable metasurface antenna based on the liquid metal for flexible scattering fields manipulation," *Micromachines*, vol. 12, no. 3, p. 243, Feb. 2021.

[20] L. Chen, Y. Ruan, and H. Y. Cui, "Liquid metal metasurface for flexible beam-steering," *Opt. Exp.*, vol. 27, no. 16, pp. 23282–23292, 2019.

[21] S. Ghosh and S. Lim, "Fluidically switchable metasurface for wide spectrum absorption," *Sci. Rep.*, vol. 8, no. 1, pp. 1–9, Jul. 2018.

[22] A. H. Naqvi and S. Lim, "A beam-steering antenna with a fluidically programmable metasurface," *IEEE Trans. Antennas Propag.*, vol. 67, no. 6, pp. 3704–3711, Jun. 2019.

[23] H. Kiani, A. Quddious, D. Chatzichristodoulou, N. Shoaib, D. Psychogiou, P. Vryonides, and S. Nikolaou, "Radiation beam steering using a microfluidically reconfigurable metasurface superstrate," in *Proc. IEEE Int. Symp. Antennas Propag., USNC-URSI Radio Sci. Meeting (AP-S/URSI)*, Jul. 2022, pp. 1642–1643, doi: 10.1109/AP-S/USNC-URSI47032.2022.9887334.

[24] S. Shah and S. Lim, "Microfluidically frequency-reconfigurable quasi-yagi dipole antenna," *Sensors*, vol. 18, no. 9, p. 2935, Sep. 2018.

[25] A. Dey, R. Guldiken, and G. Mumcu, "Microfluidically reconfigured wideband frequency-tunable liquid-metal monopole antenna," *IEEE Trans. Antennas Propag.*, vol. 64, no. 6, pp. 2572–2576, Jun. 2016.

[26] Y. Liu, Q. Wang, Y. Jia, and P. Zhu, "A frequency- and polarization-reconfigurable slot antenna using liquid metal," *IEEE Trans. Antennas Propag.*, vol. 68, no. 11, pp. 7630–7635, Nov. 2020.

[27] D. Kampouridou and A. Feresidis, "Tunable multibeam holographic metasurface antenna," *IEEE Antennas Wireless Propag. Lett.*, vol. 21, no. 11, pp. 2264–2267, Nov. 2022, doi: 10.1109/LAWP.2022.3192977.

[28] Z. Wang, S. Zhao, and Y. Dong, "Pattern reconfigurable, low-profile, vertically polarized, ZOR-metasurface antenna for 5G application," *IEEE Trans. Antennas Propag.*, vol. 70, no. 8, pp. 6581–6591, Aug. 2022, doi: 10.1109/TAP.2022.3162332.

[29] H. P. Z. Cano, Z. D. Zaharis, T. V. Yioultsis, N. V. Kantartzis, and P. I. Lazaridis, "Pattern reconfigurable antennas at millimeter-wave frequencies: A comprehensive survey," *IEEE Access*, vol. 10, pp. 83029–83042, 2022, doi: 10.1109/ACCESS.2022.3196456.

[30] P. Xie, G. Wang, H. Li, and J. Liang, "A dual-polarized two-dimensional beam-steering Fabry–Pérot cavity antenna with a reconfigurable partially reflecting surface," *IEEE Antennas Wireless Propag. Lett.*, vol. 16, pp. 2370–2374, 2017.

[31] S. I. H. Shah, A. Sarkar, R. Phon, and S. Lim, "Two-dimensional electromechanically transformable metasurface with beam scanning capability using four independently controllable shape memory alloy axes," *Adv. Opt. Mater.*, vol. 8, no. 22, Nov. 2020, Art. no. 2001180.

[32] S. I. H. Shah, A. Sarkar, and S. Lim, "Electromechanically deployable high-gain pop-up antenna using shape memory alloy and kirigami technology," *IEEE Access*, vol. 8, pp. 225210–225218, 2020.

[33] *Shape Memory Polymer Sheet—Mindsets Online*. Accessed: Aug. 7, 2023. [Online]. Available: https://mindsetsonline.co.uk/shop/shape-memory-polymer/

[34] C. Lor, R. Phon, M. Lee, and S. Lim, "Multi-functional thermal-mechanical anisotropic metasurface with shape memory alloy actuators," *Mater. Design*, vol. 216, Apr. 2022, Art. no. 110569, doi: 10.1016/J.MATDES.2022.110569.
[35] X. Huang, K. Kumar, M. K. Jawed, A. M. Nasab, Z. Ye, W. Shan, and C. Majidi, "Highly dynamic shape memory alloy actuator for fast moving soft robots," *Adv. Mater. Technol.*, vol. 4, no. 4, Apr. 2019, Art. no. 1800540, doi: 10.1002/ADMT.201800540.
[36] S. J. Mazlouman, A. Mahanfar, C. Menon, and R. G. Vaughan, "Reconfigurable axial-mode helix antennas using shape memory alloys," *IEEE Trans. Antennas Propag.*, vol. 59, no. 4, pp. 1070–1077, Apr. 2011, doi: 10.1109/TAP.2011.2109686.
[37] J. Hao, J. Ren, X. Du, J. H. Mikkelsen, M. Shen, and Y. Z. Yin, "Pattern-reconfigurable Yagi–Uda antenna based on liquid metal," *IEEE Antennas Wireless Propag. Lett.*, vol. 20, no. 4, pp. 587–591, Apr. 2021.
[38] S. I. H. Shah and S. Lim, "Thermally beam-direction- and beamwidth-switchable monopole antenna using origami reflectors with smart shape memory polymer hinges," *IEEE Antennas Wireless Propag. Lett.*, vol. 18, no. 8, pp. 1696–1700, Aug. 2019.
[39] X. L. Chang, P. S. Chee, E. H. Lim, and N.-T. Nguyen, "Frequency reconfigurable smart antenna with integrated electroactive polymer for far-field communication," *IEEE Trans. Antennas Propag.*, vol. 70, no. 2, pp. 856–867, Feb. 2022.
[40] I. T. Nassar, H. Tsang, D. Bardroff, C. P. Lusk, and T. M. Weller, "Mechanically reconfigurable, dual-band slot dipole antennas," *IEEE Trans. Antennas Propag.*, vol. 63, no. 7, pp. 3267–3271, Jul. 2015.
[41] T. Debogovic and J. Perruisseau-Carrier, "Array-fed partially reflective surface antenna with independent scanning and beamwidth dynamic control," *IEEE Trans. Antennas Propag.*, vol. 62, no. 1, pp. 446–449, Jan. 2014.
[42] R. Guzman-Quiros, J. L. Gomez-Tornero, A. R. Weily, and Y. J. Guo, "Electronically steerable 1-D Fabry–Pérot leaky-wave antenna employing a tunable high impedance surface," *IEEE Trans. Antennas Propag.*, vol. 60, no. 11, pp. 5046–5055, Nov. 2012.
[43] A. Ourir, S. N. Burokur, and A. de Lustrac, "Electronic beam steering of an active metamaterial-based directive subwavelength cavity," in *Proc. 2nd Eur. Conf. Antennas Propag. (EuCAP)*, 2007, pp. 1–4.
[44] L. Yan, P. C. Wu, Q. Song, W. Zhu, W. Zhang, D. P. Tsai, F. Capasso, and A. Q. Liu, "Dynamic beam steering in micro-fluidic-meta-surface," in *Proc. CLEO, QELS_Fundam. Sci.*, 2015, pp. 3–4.
[45] M. Kim, J. Heo, H. Rodrigue, H. Lee, S. Pané, M. Han, and S. Ahn, "Shape memory alloy (SMA) actuators: The role of material, form, and scaling effects," *Adv. Mater.*, vol. 35, no. 33, Jun. 2023, Art. no. 2208517, doi: 10.1002/ADMA.202208517.
[46] *BioMetal [TOKI Corporation]*. Accessed: Aug. 7, 2023. [Online]. Available: https://www.toki.co.jp/biometal/english/contents.php

SYED IMRAN HUSSAIN SHAH received the B.Sc. degree in telecommunication engineering and the M.S. degree in electrical engineering from the University of Engineering and Technology Peshawar, Peshawar, Pakistan, in 2011 and 2014, respectively, and the Ph.D. degree from the School of Electrical and Electronics Engineering, Chung-Ang University, Seoul, Republic of Korea, in 2020. Since March 2022, he is working as an Associate Professor with the Faculty of Electronics, Telecommunication and Informatics, Gdańsk University of Technology, Gdansk, Poland. He has authored more than 20 journals and conference papers focused on reconfigurable, deployable, printed smart antennas, and quasi-isotropic antennas. His current research interests include the design and analysis of frequency and pattern reconfigurable origami antennas, deployable origami antennas, 3-D printed antennas, and shape memory materials-based smart antennas.

SAYED SABIR SHAH received the B.Sc. degree in electronic engineering from the Department of Information, Communication and Technology, BUITEMS University, Quetta, Pakistan, and the M.S. degree in electrical engineering from the University of Engineering and Technology Peshawar (UET Peshawar), Peshawar, Pakistan, in 2019. Currently, he is a researcher in the field of antenna. His current research interests include the design and analysis of microstrip antennas, reconfigurable antennas, and metamaterials.

EIRÍKUR BERNHARÐSSON received the B.Sc. degree in mechatronics engineering from Reykjavik University, in 2022, where he is currently pursuing the B.Sc. degree in computer science. He is an Assistant Researcher for Prof. Slawomir Koziel and a Documentarian and a Rover Operator on the NASA-funded RAVEN Project led by The University of Arizona. His current research interests include robotics and automation, computer vision, control theory, and learning-based models.

SLAWOMIR KOZIEL (Fellow, IEEE) received the M.Sc. and Ph.D. degrees in electronic engineering from the Gdańsk University of Technology, Poland, in 1995 and 2000, respectively, and the M.Sc. degree in theoretical physics and the M.Sc. and Ph.D. degrees in mathematics from the University of Gdańsk, Poland, in 2000, 2002, and 2003, respectively. He is currently a Professor with the Department of Technology, Reykjavik University, Iceland. His current research interests include the CAD and modeling of microwave and antenna structures, simulation-driven design, surrogate-based optimization, space mapping, circuit theory, analog signal processing, evolutionary computation, and numerical analysis.